Quark Forward-Backward Asymmetries - Experimental Aspects

P. S. Wells

CERN
CH-1211 Geneva 23, Switzerland

Abstract

The LEP measurements for heavy quark forward-backward asymmetries are reviewed. The analysis techniques are shown to be designed so as to minimise systematic uncertainties, and the results are statistics limited.

1 Introduction

The measurements of $A_{\rm FB}^{\rm b\overline{b}}$ by the LEP experiments are of particular interest at the present time [1]. The ingredients of heavy-flavour quark forward-backward asymmetry measurements are outlined here, with emphasis on explaining how the most important aspects of the event selection and charge identification are calibrated directly from the data themselves. This reduces the systematic uncertainties, and yields a measurement that is statistics limited even when combining results using different techniques and from all four LEP experiments. Small corrections are applied to the asymmetries to derive the "pole-asymmetries". Possible theoretical uncertainties from the QCD correction are mentioned here, and were described in more detail elsewhere in this workshop [2].

The LEP/SLD heavy flavour averaging procedure also includes direct measurements of $\mathcal{A}_{\rm b}$ and $\mathcal{A}_{\rm c}$ from the left-right-forward-backward asymmetries at SLD, and partial width measurements from LEP and SLD. The forward-backward pole asymmetries are products of $\mathcal{A}_{\rm f}$ parameters: $A_{\rm FB}^{0,{\rm f}} = \frac{3}{4}\mathcal{A}_{\rm e}\mathcal{A}_{\rm f}$, and the $\mathcal{A}_{\rm f}$ parameters are related to the ratio of vector and axial-vector couplings. Together with the partial widths, which are proportional to the sum of the squares of the couplings, these measurements can be used to infer the values of vector and axial-vector couplings of the b and c-quarks to the Z.

2 Measurement strategy

The heavy-quark asymmetry measurements use Z to hadron events. In general the event is split into 2 hemispheres by the plane perpendicular to the thrust axis. The hemisphere including the outgoing electron beam is the "forward" hemisphere. Heavy

quark events are then identified in this sample, by the presence of leptons with high p and p_T [3–6], reconstructed heavy hadrons (in particular charm mesons to measure the charm asymmetry [12–14]) or via the resolvable lifetime of b and c hadrons [7–11], together with other jet properties to improve the flavour separation. The thrust axis direction is taken to be the primary quark-antiquark direction. The charge of the quark in the forward or backward hemisphere must then be identified, from the charge of tracks associated with the heavy hadron and the rest of the event. The efficiency and purity of the flavour and charge tagging, taking into account the diluting effects of B^0 mixing, are measured from the data as far as possible.

A fit to the differential cross section in bins of the polar angle of the thrust axis is performed:

$$\frac{\mathrm{d}\sigma}{\mathrm{d}\cos\theta} \propto \frac{3}{8}(1+\cos^2\theta) + A_{\mathrm{FB}}\cos\theta \tag{2.1}$$

The fit may determine $A_{\mathrm{FB}}^{\mathrm{b\overline{b}}}$, $A_{\mathrm{FB}}^{\mathrm{c\overline{c}}}$ simultaneously. These measured asymmetries are then corrected to derive the pole asymmetry.

In comparison with the measurements of lepton forward-backward asymmetries, the efficiency and purity of the flavour tags and charge determination are much less favourable. The asymmetry measurements are not simply made with the same sample as used for the partial width measurements, because the optimal working point in tag efficiency/purity to minimise the experimental error is different.

More details on each aspect of the analysis are given in the following sections

3 Heavy flavour tags

3.1 Leptons

The first heavy-flavour analyses at LEP used identified leptons in hadronic events to tag b and c-quark events. The semileptonic branching ratio of b and c hadrons is about 20%. Electrons are identified from the characteristic ionisation in the detector tracking chambers, $\mathrm{d}E/\mathrm{d}x$, from the ratio of the energy deposited in the electromagnetic calorimeter to the track momentum, $E/p \approx 1$, and from the calorimeter shower shape. Muons are selected by requiring a match between an extrapolated track from the central tracking volume and a track segment in the muon chambers surrounding the experiment.

The lepton p and p_T, together with properties of the associated jet and lifetime information, are used for flavour separation.

3.2 Lifetimes

The average B hadron lifetime is about 1.5 ps with a typical energy of about 30 GeV, giving a decay length of 3 mm. The B decay has a charged multiplicity of about 5. The micro-vertex detectors at the centre of the experiment tracking volumes cover radii of 6–10 cm, with an impact parameter resolution of around 20μm.

Lifetime tagging variables are built up using for example the probabilities or weights for tracks to be associated to a primary or secondary vertex, the χ^2 of fits constraining charged tracks to originate either all from the primary, or from a primary and secondary vertex, the decay length of a secondary vertex and its error, and the invariant mass of

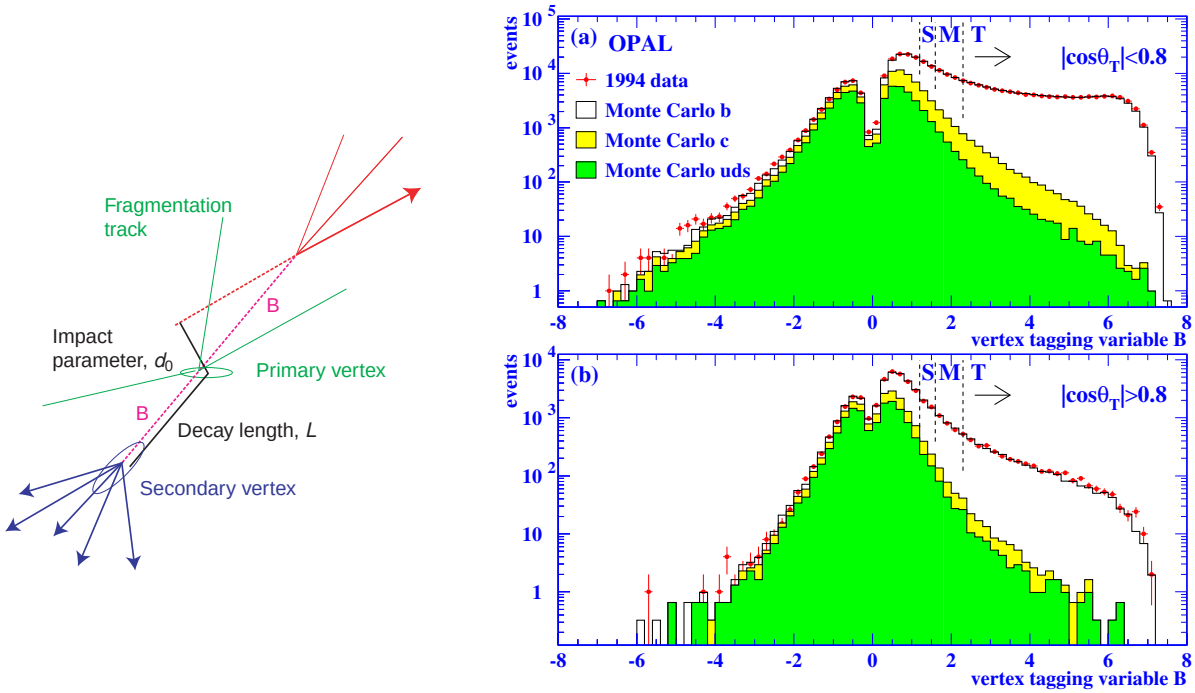

Figure 1: The relationship between tracks in an event and the lifetime tagging variables (left). Distribution of a multivariate tagging variable from OPAL (right). Regions of different purity that are used in the asymmetry analysis are indicated.

tracks associated with a secondary vertex. The impact parameter and decay length of tracks originating from a secondary vertex are indicated in Figure 1.

In practice, several flavour separation variables are combined into an overall hemisphere tag. The combinations use artificial neural networks or likelihood techniques. Different ranges of values of the tagging variable have different purities. This can be used to weight events accordingly. Very high b-purity (80-95%) can be achieved, with the dominant background coming from misidentifed charm events. The clear separation of b events using a multivariate tag can be seen in the example in Figure 1. Vertices reconstructed with negative decay lengths are given a negative value of the tagging variable, and are used to check the modelling of the experimental track resolution.

4 Charge determination

Having identified a subsample enriched in heavy flavours, the distinction between forward and backward events relies on determining the charge of the quark or antiquark in each event hemisphere. The fractions of correct tags are accounted for by the fitting techniques described in Section 5.

4.1 Leptons and other final state particles

Reconstructed hadrons and the charges of identified leptons or final state kaons distinguish between decaying quarks and antiquarks. Complications arise from $B^0\overline{B^0}$ mixing

and the presence of "cascade" decays, which unlike the prompt $b \to \ell^-$ decays, give the wrong sign lepton: $b \to c \to \ell^+$.

4.2 Inclusive charge determination

The charge of the primary quark can be inferred from the "jet charge", a momentum weighted sum of the charges of tracks associated with a jet:

$$Q_{\rm jet} = \frac{\sum_{{\rm tracks},i} p_{\parallel,i}^{\kappa} q_i}{\sum_{{\rm tracks},i} p_{\parallel,i}^{\kappa}}$$

Different values of κ are appropriate for B^0 ($\kappa \approx 0$) or B^+ ($\kappa \approx 1$) decays.

The vertex charge is a similar weighted sum of track charges, this time using the probability for tracks to have come from a reconstructed secondary vertex, rather than the primary event vertex.

$$Q_{\rm vertex} = \sum_{{\rm tracks},i} w_i^{\rm sec/prim} q_i$$

The performance of a vertex charge is illustrated in figure 2.

A multivariate charge tag can be constructed using a neural network, including one or more jet charges with different values of κ, the vertex charge and its uncertainty, and the charge of identified kaons. DELPHI include the relative probabilities that the hemisphere contained a B^0, B^+, B_s, b-baryon, and the charge of identified leptons. ALEPH and OPAL prefer to treat leptons as ordinary tracks in the inclusive tag analyses, so as to reduce the statistical correlation with the lepton fits.

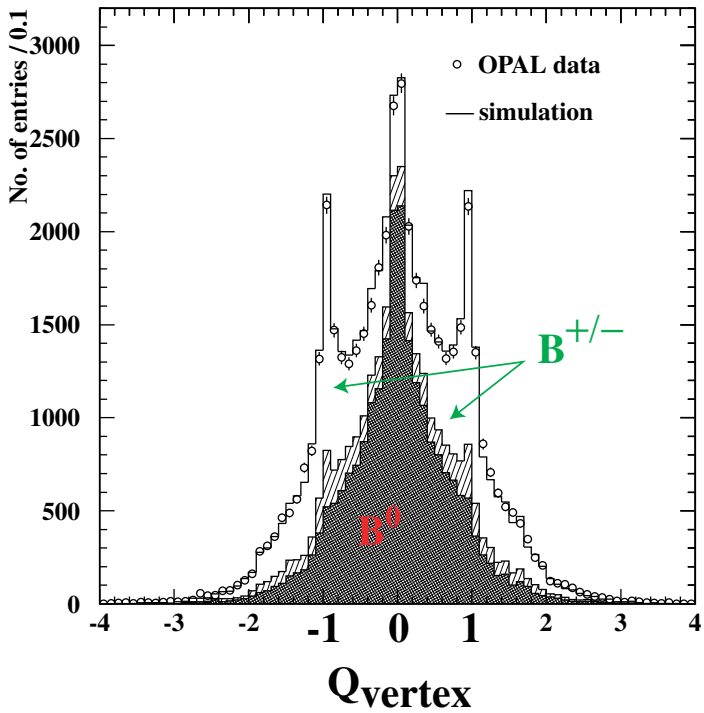

Figure 2: Distribution of vertex charges, showing peaks from B^0 and B^+ mesons.

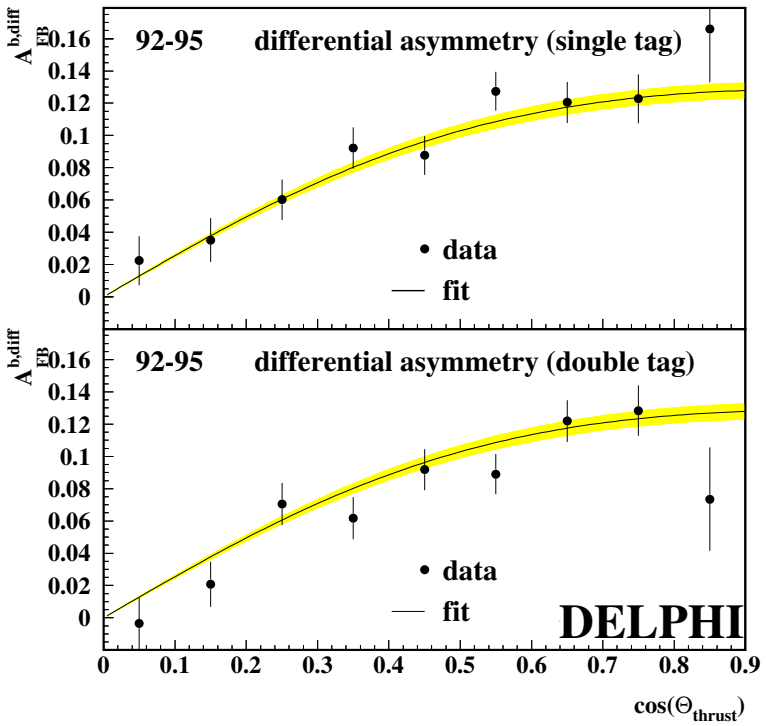

Figure 3: Result of the asymmetry fit for the DELPHI inclusive analysis.

5 Fitting methods

In general, the experiments perform fits in many bins of b-tag purity and $\cos\theta$ of the thrust axis. All the fits assume the simple differential cross section given in Eq. 2.1. An example of the data quality is shown in Figure 3, which shows the *differential asymmetry*, i.e. the asymmetry in bins of $\cos\theta$. The data are not sufficiently precise to be able to fit more free parameters to determine more exactly the differential cross section.

The flavour fractions in each bin are calibrated from the data, usually by a double tag method, which is explained below. The performance of the production charge determination is also calibrated from data. ALEPH, L3 and OPAL use the variable $\langle Q_{\rm F} - Q_{\rm B}\rangle$ as a measure of the forward backward asymmetry, while DELPHI use a double tag method to calibrate the charge mis-tag rate from the relative rates of like-sign and unlike-sign events. Systematic uncertainties enter via the residual model dependence. In particular, correlations between tag rates and charge determination between the hemispheres are taken from Monte Carlo simulation, and must be controlled.

5.1 Fits with lepton tag samples

The probable quark flavour of events with a lepton candidate has traditionally been derived from the lepton p and p_T. The flavour separation is improved using additional jet shape and lifetime variables. The observed asymmetry in any bin of flavour separating variables is then given by an expression like this, where leptons from $\mathrm{c\overline{c}}$ events and cascade decays contribute with the "wrong" sign:

$$A_{\rm FB}^{\rm obs} = f_{\rm b\ell} A_{\rm FB}^{\rm b\overline{b}}(1-2\overline{\chi}) - f_{\rm c\ell} A_{\rm FB}^{\rm c\overline{c}} - f_{\rm bc\ell} A_{\rm FB}^{\rm b\overline{b}}(1-2\overline{\chi}) + f_{\rm bkg} A_{\rm FB}^{\rm bkg}$$

The fractions f of each contribution will be different in different bins. The mixing parameter $\overline{\chi}$ dilutes the b asymmetry, but also affects the fraction of like-sign dilepton events. A fit to single and dilepton samples can therefore determine $A_{\rm FB}^{\rm b\overline{b}}$, $A_{\rm FB}^{\rm c\overline{c}}$ and $\overline{\chi}$. simultaneously.

5.2 Double tag method for purities

The double tag method was first used to measure partial widths [15], but is also a central ingredient of the asymmetry measurements, where it is used to measure the most significant tagging efficiencies directly from the data. The method relies on counting the fraction of *hemispheres* that are tagged, f_s, and fraction of *events* with a tag in both hemispheres, f_d. There may be one or more tagging variables, so the double tags can have a different tag in each hemisphere. For tags i, k, l, the fraction are given by:

$$\begin{aligned} f_s^i &= \epsilon_{\rm b}^i R_{\rm b} + \epsilon_{\rm c}^i R_{\rm c} + \epsilon_{\rm uds}^i (1 - R_{\rm b} - R_{\rm c}) \,, \\ f_d^{kl} &= \epsilon_{\rm b}^k \epsilon_{\rm b}^l D_{\rm b}^{kl} R_{\rm b} + \epsilon_{\rm c}^k \epsilon_{\rm c}^l D_{\rm c}^{kl} R_{\rm c} + \epsilon_{\rm uds}^k \epsilon_{\rm uds}^l (1 - R_{\rm b} - R_{\rm c}) \,. \end{aligned}$$

The correlations of tagging probability between hemispheres must be taken into account:

$$D_f^{kl} = \epsilon_f^{kl} / (\epsilon_f^k \epsilon_f^l).$$

These arise from such effects as the interplay between detector geometry and the typically back-to-back structure of the events, the fact that the primary vertex is common to both hemispheres, and correlations between the primary hadron momenta due to gluon radiation. The system of equations can be solved for data, taking minimum input from MC, usually the correlations and the lowest efficiencies.

5.3 The $\langle Q_{\rm F} - Q_{\rm B} \rangle$ method

While DELPHI also use a double tag method to infer the charge tagging efficiency, the other experiments examine the variable $Q_{\rm F} - Q_{\rm B}$, which is the difference between the any charge tag value Q in the forward and backward hemispheres. An example distribution is shown in Figure 4.

The average value, $\langle Q_{\rm F} - Q_{\rm B} \rangle$, is simply related to the forward-backward asymmetry. Considering only b quarks, in a particular bin of $\cos\theta$:

$$\langle Q_{\rm FB}^b \rangle \equiv \langle Q_{\rm F}^b - Q_{\rm B}^b \rangle = \frac{1}{n_{\rm tot}^b} \left(n_{\rm F}^b \langle Q_b - Q_{\overline{b}} \rangle + n_{\rm B}^b \langle Q_{\overline{b}} - Q_b \rangle \right) = \delta_b A_{\rm FB}^{\rm b\overline{b}} \frac{8}{3} \frac{\cos\theta}{1 + \cos^2\theta}$$

The asymmetry is diluted by the *charge separation* $\delta_b = \langle Q_b - Q_{\overline{b}} \rangle$. Including all quark flavours, writing $s_f = \pm 1$ for down/up-type quarks and P_f as the fraction of flavour f:

$$\langle Q_{\rm FB} \rangle = \sum_f s_f P_f \delta_f A_{\rm FB}^{\rm f\overline{f}} \frac{8}{3} \frac{\cos\theta}{1 + \cos^2\theta}$$

The fractions P_f are found using the double tag method. The other essential ingredient, the charge separation can also be derived from the data, because it is closely related to the average value of the product of the two hemisphere charges. Again, corrections for hemisphere correlations must be made. The value of $A_{\rm FB}^{\rm b\overline{b}}$ can then be obtained from a fit in bins of flavour tagging variables and $\cos\theta$.

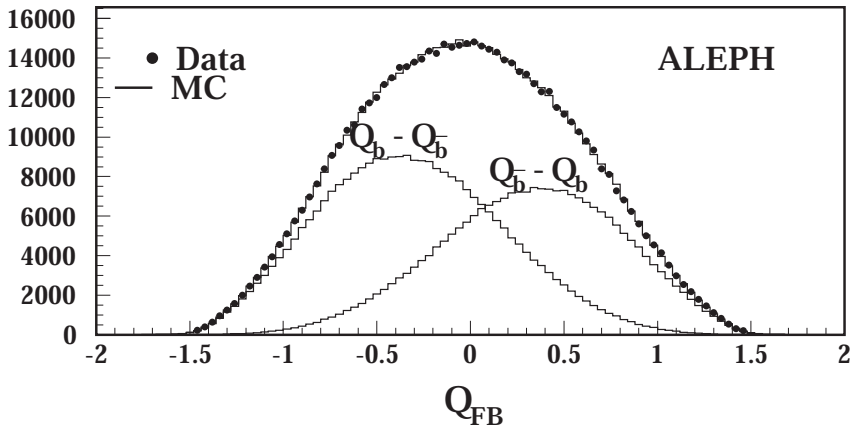

Figure 4: The distribution of $Q_{\mathrm{F}} - Q_{\mathrm{B}}$ in a b-rich sample from a multivariate flavour tag. Vertex, jet and kaon charges are combined into a charge neural net.

5.4 Systematic uncertainties

By measuring as much as possible from the data, the results remain statistics limited. Uncertainties in the Monte Carlo modelling feed into the analysis via those quantities still taken from simulation, such as hemisphere correlations. These uncertainties include b and c fragmentation functions, knowledge of b and c hadron decay properties, detector resolution effects on the efficiencies for charm and light quark backgrounds, and modelling of detector material asymmetries and/or magnetic field effects that cause asymmetries in the number of positive and negative tracks. To control the hemisphere correlations, the underlying variables that contribute to the correlation must be identified. These variables may not be directly measurable in the data, so experimental observables that are closely related are studied in data and Monte Carlo simulation, to assess the range of correlation that is consistent with the data.

There are also common theoretical uncertainties from the corrections to go from the measured asymmetries to the pole asymmetries, discussed in section 6.2.

6 Results

6.1 Heavy Flavour Averaging Procedure

All the heavy flavour results are combined in a χ^2 minimisation procedure which simultaneously determines the average values of R_{b}, R_{c}, the asymmetries, and some auxiliary parameters which are determined by closely related measurements [16]. The full covariance matrix between the measurements is calculated, taking into account statistical correlations and common systematic uncertainties. The *experimental* interdependences are taken into account: for example, the forward-backward asymmetry measurements depend on the fractions R_{b} and R_{c}. But the SM relationships between the parameters are in general not imposed, apart from the centre-of-mass energy dependence of the forward-backward asymmetries. A first fit is performed assuming that the on and off-peak forward-backward asymmetries are independent results. The results are shown in

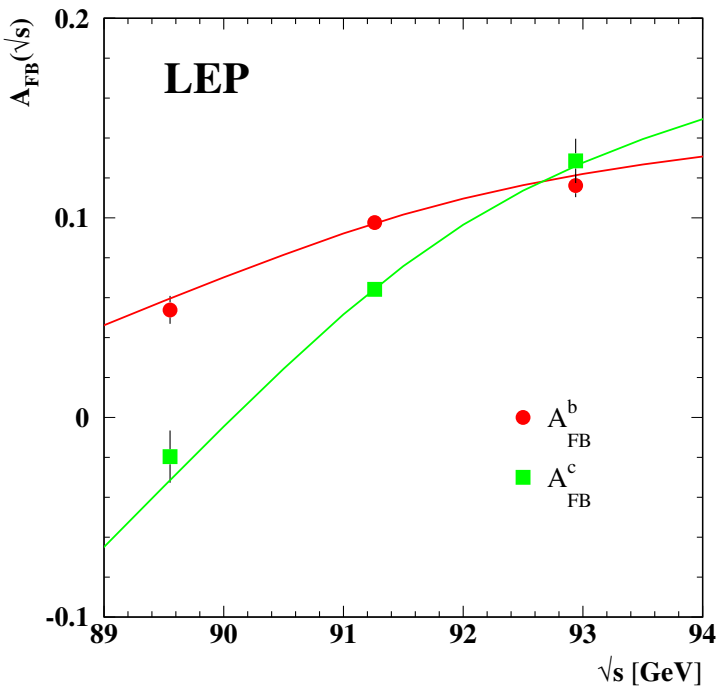

Figure 5: Centre-of-mass energy dependence of the LEP average forward-backward asymmetry measurements.

Figure 5. After verifying that the energy dependence of the asymmetries follows the Standard Model expectation, a second fit is performed where all the forward-backward asymmetries are corrected to pole asymmetries.

The statistical correlations between the inclusive and lepton-tag measurements are quoted as 0.264 ± 0.039 by ALEPH, 0.30 (preliminary) by DELPHI, 0.06 for L3 and 0.35 (preliminary) by OPAL. The low L3 number is because only p and p_T are used for flavour separation, and no lepton identification is used as a tag in the inclusive analysis. DELPHI allow more overlap of tagging information between the lepton and inclusive measurements, but the relative precision of the two measurements is different for different experiments, and the quoted DELPHI correlation turns out to be similar in size to that of ALEPH and OPAL.

6.2 Corrections to obtain pole asymmetries

The asymmetries are corrected for the centre-of-mass energy dependence to give the equivalent value at $\sqrt{s} = m_{\mathrm{Z}}$ using ZFITTER [17] v.6.35 with $m_{\mathrm{Z}} = 91.1875$ GeV, $m_{\mathrm{t}} = 175$ GeV $m_{\mathrm{H}} = 100$ GeV and $\alpha_{\mathrm{S}} = 0.12$. ZFITTER is also used to calculate small shifts in $A_{\mathrm{FB}}^{\mathrm{b\bar{b}}}$ due to ISR ($+0.0041$), photon exchange and γ-Z interference and b quark mass effects (-0.0003).

The QCD correction leads to the largest common systematic uncertainty. It is expressed as [15, 18]

$$A_{\mathrm{FB}}^{\mathrm{b\bar{b}},\mathrm{meas}} = (1 - s_{\mathrm{bias}} C_{\mathrm{QCD}}^{\mathrm{b}}) A_{\mathrm{FB}}^{\mathrm{b\bar{b}},\mathrm{noQCD}}$$

Experimentally the quark direction is estimated by the hadron level thrust axis. QCD corrections are calculated to 1st order with mass corrections, and 2nd order for massless quarks, using the parton thrust axis. The correction to hadron level is assessed using Monte Carlo, and the full parton to hadron shift is assigned as an error.

$$C_{\rm QCD}^{\rm b} = C_{\rm analytic}^{\rm parton-thrust} + \langle C_{\rm MC}^{\rm hadron-thrust} - C_{\rm MC}^{\rm parton-thrust} \rangle$$

The experimental factor $s_{\rm bias}$ is also calculated from Monte Carlo simulation, and reflects the fact that the experimental methods reduce the overall impact of the QCD effects. In particular, the flavour tags are more efficient for higher energy hadrons, reducing the energy available for gluon radiation. Calibrating the charge tagging efficiency from data also tends to calibrate out QCD effects.

$$A_{\rm FB}^{\rm b\overline{b},MCmeas} = (1 - s_{\rm bias} C_{\rm MC}^{\rm hadron-thrust}) A_{\rm FB}^{\rm b\overline{b},MCnoQCD}$$

Value of $C_{\rm QCD}$	$\rm b\overline{b}$	$\rm c\overline{c}$
	0.0354	0.0413
Error on $C_{\rm QCD}$	$\rm b\overline{b}$	$\rm c\overline{c}$
Higher orders	0.0025	0.0046
Error on quark mass	0.0015	0.0008
Higher order mass effects	0.005	0.002
$\alpha_{\rm S} = 0.0119 \pm 0.003$	0.0012	0.0015
MC parton to hadron	0.0023	0.0035
Total error	0.0063	0.0063

Table 1: The total QCD correction and a breakdown of the systematic uncertains assumed.

The correction and error are scaled by the value of $A_{\rm FB}^{\rm b\overline{b}}$. The correction is further reduced by $\approx 50\%$ on average by $s_{\rm bias}$. There is still some discussion over whether the error should also be scaled by the full $s_{\rm bias}$ factor.

6.3 LEP plus SLD combined heavy flavour results

Correcting the forward-backward asymmetries on and off-peak to give pole asymmetries, including LEP measurements of $R_{\rm b}$ and $R_{\rm c}$, and the preliminary SLD results for $R_{\rm b}$, $R_{\rm c}$, $\mathcal{A}_{\rm b}$ and $\mathcal{A}_{\rm c}$ [15], the combined fit gives the following average values:

$$\begin{aligned}
R_{\rm b}^0 &= 0.21644 \pm 0.00065\,, \\
R_{\rm c}^0 &= 0.1718 \pm 0.0031\,, \\
A_{\rm FB}^{0,\rm b} &= 0.0995 \pm 0.0017\,, \\
A_{\rm FB}^{0,\rm c} &= 0.0713 \pm 0.0036\,, \\
\mathcal{A}_{\rm b} &= 0.922 \pm 0.020\,, \\
\mathcal{A}_{\rm c} &= 0.670 \pm 0.026\,.
\end{aligned}$$

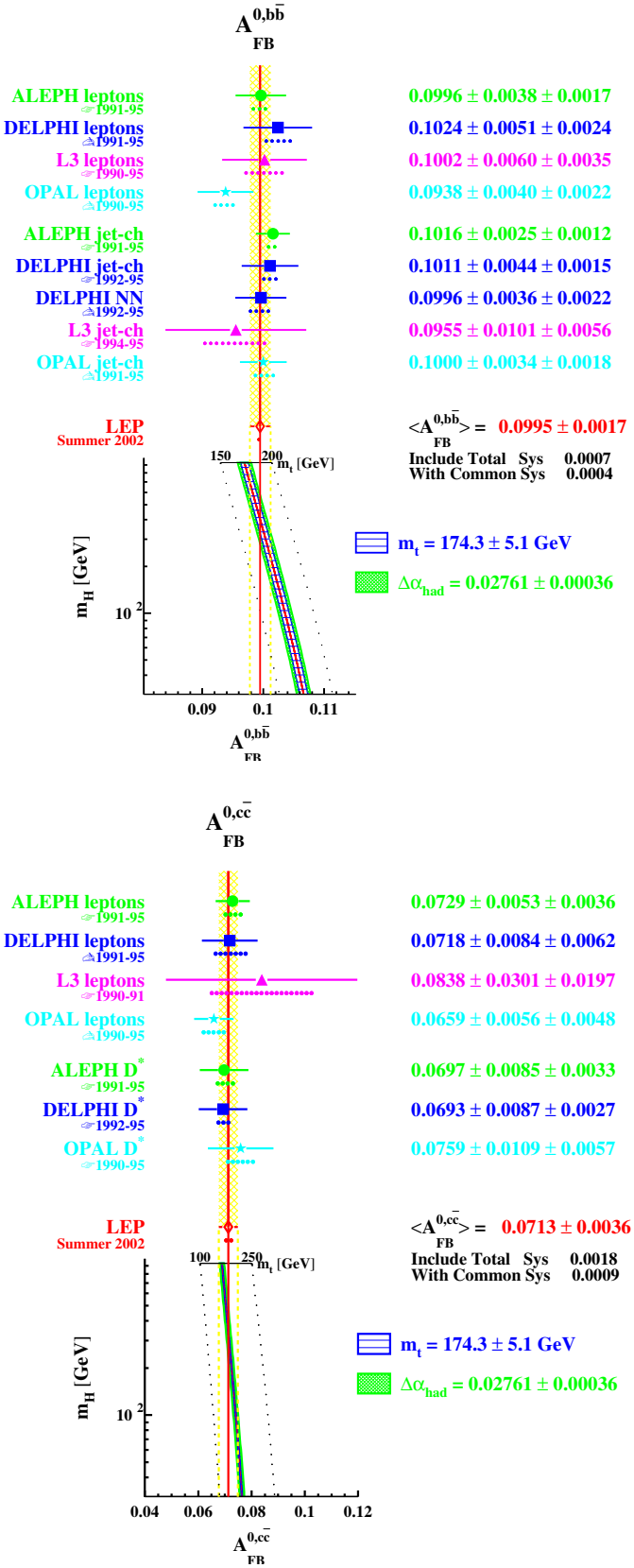

Figure 6: Results for $A_{\rm FB}^{0,\,\rm b}$ and $A_{\rm FB}^{0,\,\rm c}$.

The fit has a low $\chi^2 = 47.6$ for (105-14) d.o.f., (probability 0.99995), suggesting that the errors may be over estimated. Using statistical errors only, gives a χ^2 of 85.2 for (105-14) d.o.f. The low χ^2 is not limited to any particular category of measurements.

The individual experimental results for $A_{\rm FB}^{0,\,\rm b}$ and $A_{\rm FB}^{0,\,\rm c}$ are listed in Figure 6. Both averages are statistics limited. For $A_{\rm FB}^{0,\,\rm b}$, the total systematic error is 0.00068, of which 0.00040 is common to all the experiments, and 0.00035 is the due to the QCD correction uncertainty. The charm result has a slightly higher systematic component of 0.0018. The result is rather less precise than $A_{\rm FB}^{0,\,\rm b}$ and in addition is less sensitive to $\sin^2\theta_{\rm eff}^{\rm lept}$. Comparisons of the inferred values of $\sin^2\theta_{\rm eff}^{\rm lept}$ and $\mathcal{A}_{\rm f}$ were shown elsewhere in this workshop [1]. The partial width measurements are in good agreement with the Standard Model expectation.

7 Conclusions

Because the analyses are structured to minimise systematic uncertainties, the quark forward-backward asymmetry results from LEP1 are statistically limited. The largest systematic error comes from the treatment of QCD corrections, where the uncertainty is thought to be conservative.

No major changes are foreseen in the near future. The results of ALEPH and L3 are final. DELPHI expect to improve the precision of their inclusive tag measurement shortly, and to finalise their lepton tag result. OPAL also expect some improvement in the precision of their lepton tag result. There may be marginal changes to ensure a uniform treatment of the QCD correction uncertainty, and the uncertainty in statistical correlations.

The heavy flavour results from SLD agree with the predictions of the Standard Model, and do not shed light on the pull of $A_{\rm FB}^{0,\,\rm b}$ in global electroweak fits [1].

From an experimental point of view, the quark asymmetry measurements seem to be robust. Perhaps a future linear collider will be able to devote time to running at the Z with high luminosity, and resolve the question of whether this tantalising deviation is a hint of new physics in the b sector, or merely a statistical fluctuation.

References

[1] M. Grünewald, these proceedings.

[2] W. van Neerven, these proceedings.

[3] ALEPH Collaboration, A. Heister, *et al.*, Eur. Phys. J. **C24** (2002) 177.

[4] DELPHI Collaboration, P.Abreu *et al.*, Z. Phys **C65** (1995) 569;
DELPHI Collaboration, *Measurement of the Forward-Backward Asymmetries of* $e^+e^- \to Z \to b\overline{b}$ *and* $e^+e^- \to Z \to c\overline{c}$ *using prompt leptons* DELPHI 2002-028-CONF-562, contributed paper to ICHEP 2002 Amsterdam.
Delphi notes are available at http://wwwcn.cern.ch/~pubxx/www/delsec/delnote/.

[5] L3 Collaboration, O. Adriani *et al.*, Phys. Lett. **B292** (1992) 454;
L3 Collaboration, *L3 Results on* $A_{\rm FB}^{\rm b\overline{b}}$, $A_{\rm FB}^{\rm c\overline{c}}$ *and* χ *for the Glasgow Conference,* L3

Note 1624;
L3 Collaboration, M. Acciarri *et al.*, Phys. Lett. **B448** (1999) 152.

[6] OPAL Collaboration, G. Alexander *et al.*, Z. Phys. **C70** (1996) 357;
OPAL Collaboration, R. Akers *et al.*, *Updated Measurement of the Heavy Quark Forward-Backward Asymmetries and Average B Mixing Using Leptons in Multihadronic Events*, OPAL Physics Note PN226 contributed paper to ICHEP96, Warsaw, 25-31 July 1996 **PA05-007**
OPAL Collaboration, R. Akers *et al.*, *QCD corrections to the bottom and charm forward-backward asymmetries* OPAL Physics Note PN284.

[7] ALEPH Collaboration, A. Heister *et al.*, Eur. Phys. J. **C22** (2001) 201.

[8] DELPHI Collaboration, P.Abreu *et al.*, Eur. Phys. J. **C9** (1999) 367.

[9] DELPHI Collaboration, *Determination of A_{FB}^b using inclusive charge reconstruction and lifetime tagging at LEP 1*, DELPHI 2001-048 CONF 476.

[10] L3 Collaboration, M. Acciarri *et al.*, Phys. Lett. **B439** (1998) 225.

[11] OPAL Collaboration, G. Abbiendi *et al.*, Phys. Lett. **B546** (2002) 29.

[12] ALEPH Collaboration, R. Barate *et al.*, Phys. Lett. **B434** (1998) 415.

[13] DELPHI Collaboration, P.Abreu *et al.*, Eur. Phys. J. **C10** (1999) 219.

[14] OPAL Collaboration, G. Alexander *et al.*, Z. Phys. **C73** (1996) 379.

[15] *A Combination of Preliminary Electroweak Measurements and Constraints on the Standard Model*, The LEP Collaborations, ALEPH, DELPHI, L3, OPAL, the LEP Electroweak Working Group, and the SLD Heavy Flavour Group, CERN-EP/2002-091, hep-ex/0212036, 17th December 2002, and references therein.

[16] The LEP Experiments: ALEPH, DELPHI, L3 and OPAL, Nucl. Inst. Meth. **A378** (1996) 101.

[17] D. Bardin *et al.*, Z. Phys. **C44** (1989) 493; Comp. Phys. Comm. **59** (1990) 303; Nucl. Phys. **B351**(1991) 1; Phys. Lett. **B255** (1991) 290 and CERN-TH 6443/92 (May 1992); the most recent version of ZFITTER (6.21) is described in DESY 99-070, hep-ph/9908433 (Aug 1999) published in Comp. Phys. Comm. **133** (2001) 229.

[18] D. Abbaneo *et al.*, Eur. Phys. J. **C4** (1998) 185.